
1
2 **Morphogenesis as Bayesian Inference:**
3 **A Variational Approach to Pattern Formation and Control in**
4 **Complex Biological Systems**

5
6 Franz Kuchling¹, Karl Friston², Georgi Georgiev³, Michael Levin^{1*}

7 **1** Biology Department, Allen Discovery Center at Tufts University, Medford, MA, USA

8 **2** The Wellcome Trust Centre for Neuroimaging, Institute of Neurology, Queen Square,
9 London, UK

10 **3** Assumption College, Department of Physics, 500 Salisbury St., Worcester, MA, USA

11 * Michael.Levin@tufts.edu

12 **1 Abstract**

13 Recent advances in molecular biology such as gene editing [Mahas et al., 2018],
14 bioelectric recording and manipulation [Levin, 2012a] and live cell microscopy using
15 fluorescent reporters [Mutoh et al., 2012], [V. Sekar et al., 2011] – especially with the
16 advent of light-controlled protein activation through optogenetics [Bugaj et al., 2017] –
17 have provided the tools to measure and manipulate molecular signaling pathways with
18 unprecedented spatiotemporal precision. This has produced ever increasing detail about
19 the molecular mechanisms underlying development and regeneration in biological
20 organisms. However, an overarching concept – that can predict the emergence of form
21 and the robust maintenance of complex anatomy – is largely missing in the field.
22 Classic (i.e., dynamic systems and analytical mechanics) approaches such as least action
23 principles are difficult to use when characterizing open, far-from equilibrium systems
24 that predominate in Biology. Similar issues arise in neuroscience when trying to
25 understand neuronal dynamics from first principles. In this (neurobiology) setting, a
26 variational free energy principle has emerged based upon a formulation of
27 self-organization in terms of (active) Bayesian inference. The free energy principle has
28 recently been applied to biological self-organization beyond the neurosciences [Friston
29 et al., 2015], [Friston, 2013]. For biological processes that underwrite development or
30 regeneration, the Bayesian inference framework treats cells as information processing
31 agents, where the driving force behind morphogenesis is the maximization of a cell’s
32 model evidence. This is realized by the appropriate expression of receptors and other
33 signals that correspond to the cell’s internal (i.e., generative) model of what type of
34 receptors and other signals it should express. The emerging field of the free energy
35 principle in pattern formation provides an essential quantitative formalism for
36 understanding cellular decision-making in the context of embryogenesis, regeneration,
37 and cancer suppression. In this paper, we derive the mathematics behind Bayesian
38 inference – as understood in this framework – and use simulations to show that the
39 formalism can reproduce experimental, top-down manipulations of complex
40 morphogenesis. First, we illustrate this ‘first principle’ approach to morphogenesis
41 through simulated alterations of anterior-posterior axial polarity (i.e., the induction of
42 two heads or two tails) as in planarian regeneration. Then, we consider aberrant
43 signaling and functional behavior of a single cell within a cellular ensemble – as a first
44 step in carcinogenesis as false ‘beliefs’ about what a cell should ‘sense’ and ‘do’. We
45 further show that simple modifications of the inference process can cause – and rescue –
46 mis-patterning of developmental and regenerative events without changing the implicit
47 generative model of a cell as specified, for example, by its DNA. This formalism offers a
48 new road map for understanding developmental change in evolution and for designing
49 new interventions in regenerative medicine settings.

2 An Introduction to Bayesian Inference

Evolutionary change results from mutations in DNA and selection acting on functional bodies. Thus, it is essential to understand how the hardware encoded by the genome enables the behavioral plasticity of cells that can cooperate to build and repair complex anatomies. Indeed, most problems of biomedicine – repair of birth defects, regeneration of traumatic injury, tumor reprogramming, *etc.* – could be addressed if prediction and control could be gained over the processes by which cells implement dynamic pattern homeostasis. The fundamental knowledge gap and opportunity of the next decades in the biosciences is to complement bottom-up molecular understanding of mechanisms with a top-down computational theory of cellular decision-making and infotaxis. Relevant concepts have been developed in neuroscience and physics, but are generally not familiar to developmental or regenerative biologists [Friston et al., 2015], [Friston, 2013]. Here, we lay out the mathematical foundation of the type of Bayesian modeling employed by new approaches to understand metazoan cell cooperation to characterize – and simulate – pattern formation. We start by identifying a Lyapunov function that can be used to analyze and solve any dynamic system, using the fundamental theorem of vector calculus (i.e., the Helmholtz Decomposition). We use it to characterize the generalized flow of systemic states, in terms of convergence to a non-equilibrium steady-state. We then introduce the notion of a Markov blanket that separates the external and internal states of the system, where the Markov blanket is comprised of active and sensory states. Using this partition, we can then replace the Lyapunov function with a variational free energy to solve for the evolution of internal and active states and thereby characterize self-organization in far from equilibrium systems that can be partitioned into a cell (i.e., internal states and their Markov blanket) and the external milieu. Subsequent sections apply this formalism to illustrate morphogenesis and neoplasia using simulations. Bayesian inference is a statistical process, wherein Bayes theorem is used to update the probability of a hypothesis with respect to evidence obtained by measurement of the sensorium – or environment. In essence, any kind of information processing system infers unobservable (i.e., hidden) states of its environment by comparing sensory samples with predictions of sensory input and updating its expectations about the causes of that input. Bayes theorem rests on the three basic axioms of probability theory and is used to relate the conditional probability of an unobservable event A, given an observable quantity B, to the likelihood of B, given that A is true. This is written as:

$$P(A | B) = \frac{P(B | A)P(A)}{P(B)}, \quad (1)$$

where conditional probability $P(A | B)$ is also called the *posterior*; namely, the inferred probability of an event A, given an event B. Conversely, $P(B | A)$ is the probability of B, given A, called the *likelihood*. The probability $P(A)$ is called a *prior* belief and the probability of $P(B)$, is called marginal likelihood or *evidence*. In Bayesian inference, the above relationship is used to accumulate information about an unobservable or hidden state by sampling measurable events. This is known as Bayesian belief updating, because it converts prior beliefs into posterior beliefs – based on a generative model. This is known as Bayesian belief updating that is used to update the agent’s prior beliefs based on its *generative model*, $P(A | B) = P(B | A)P(A)$. In short, the likelihood assigned to the observation and prior beliefs are combined to form posterior beliefs.

To describe the dynamics of an ensemble of information processing agents (as in cells, for example) as a process of Bayesian belief updating, we need to relate the stochastic differential equations governing Newtonian motion and biochemical activity

98 to the probabilistic quantities above. This is fairly straightforward to do, if we associate
99 biophysical states with the parameters of a probability density – and ensure their
100 dynamics perform a gradient flow on a quantity called variational free energy.

101 Variational free energy is a quantity in Bayesian statistics that, when minimized,
102 ensures the parameterized density converges to the posterior belief, as we will see below.

103 In neuroscience, the minimization of variational free energy is referred to as active
104 inference. This approach to neuronal dynamics has been successfully used to reproduce
105 a variety of neuronal phenomena [Friston et al., 2017], [Ungerleider and Leslie,
106 2000], [Adams et al., 2013], [Desimone and Duncan, 1995], [Barrett and Simmons,
107 2015], [Corbetta and Shulman, 2002]. Crucially, exactly the same scheme has been
108 shown recently – through computational proof-of-principle simulations – to produce and
109 maintain the somatic patterning of self-organization [Friston, 2013], [Friston et al., 2015].
110 We will see that when the basic condition for an inference type description of a system –
111 namely, the existence of a Markov blanket separating external and internal states – is
112 satisfied, agents such as biological cells form into organized conglomerations based on
113 their generative models of how of their blanket states influence – and are influenced by –
114 external states in the external milieu (i.e., the states of other cells) [Friston, 2013].

115 In classical thermodynamic descriptions, this would be accompanied by an increase
116 of thermodynamic entropy over the entire system, through localized increases in
117 organization (i.e., decrease in entropy) of the states associated with each cell (i.e.,
118 internal states and their Markov blanket). However, as biological systems, especially
119 cells, are invariably open, far-from-equilibrium or non-equilibrium steady state systems,
120 the dynamics of this process are almost impossible to compute. Instead, by focusing on
121 a probabilistic account of self-organization, in terms of Bayesian belief updating, we can
122 place an upper bound on the entropy of the system’s blanket states that is
123 computationally tractable. In brief, we will see that the dynamics of system with a
124 Markov blanket that self-organizes to non-equilibrium steady-state can be described as
125 a gradient flow on this computable (variational) free energy bound. This approach has
126 been shown to have a high predictive validity in neurobiology; both in terms of behavior
127 and the neuronal correlates of action and perception. However, its application in the
128 broader biosciences has not been explored, even though the basic assumptions behind it
129 apply broadly.

130 3 Mathematical Foundations

131 In what follows, we introduce the mathematics that underwrites the Bayesian
132 interpretation of non-equilibrium steady-state dynamics. We will start with a brief
133 overview of the Helmholtz decomposition and Lyapunov functions in dynamical systems.
134 We will see that one can formulate any dynamics in terms of a potential function that
135 plays the role of a Lyapunov function. This is illustrated from the point of view of
136 classical mechanics with dissipative aspects. We then derive the same result in terms of
137 density dynamics using the Fokker Planck equation, in generalized coordinates of
138 motion. This formulation shows that the potential or Lyapunov function is simply the
139 negative log probability of a state being occupied at non-equilibrium steady-state.
140 Crucially, this quantity is bounded from above by variational free energy. This means
141 the flow of particular states at non-equilibrium steady-state can be cast as a gradient
142 flow on the same quantity that is minimized by Bayesian belief updating.

143 3.1 Stability and Convergence in Coupled Dynamical Systems

144 3.1.1 The Helmholtz decomposition

145 The Helmholtz decomposition states that any sufficiently smooth (i.e., possessing
146 continuous derivatives) vector field \mathbf{F} can be decomposed into an irrotational (curl-free)
147 and a solenoidal (divergence-free) vector field. Because an irrotational vector field has
148 only a scalar potential and a solenoidal vector field has only a vector potential, we can
149 express the vector field as

$$\mathbf{F} = -\nabla\Phi + \nabla \times \mathbf{A}, \quad (2)$$

150 where $\nabla\Phi$ and $\nabla \times \mathbf{A}$ are the irrotational and solenoidal vector fields respectively.

151 3.1.2 Lyapunov functions

152 Lyapunov functions have been used extensively in dynamical systems theory and
153 engineering to characterize the stability of fixed points of a dynamical
154 system [Lyapunov, 1992], [Mawhin, 2015]. Lyapunov functions are generally defined for
155 smooth systems through the following conditions:

$$\begin{aligned} (a) \quad & L(x^*) = 0, \text{ and } L(x) > 0 \text{ if } x \neq x^* \\ (b) \quad & \dot{L}(x) = \left. \frac{dL}{dt} \right|_x \leq 0, \text{ for all } x \in O, \end{aligned} \quad (3)$$

156 where $O \subseteq \mathbb{R}$ is an open set containing all states x .

157 (a) requires the Lyapunov function L to be minimal for fixed points x^* representing
158 local minima, and (b) denotes convergence to these fixed points over time.
159 Following [Yuan et al., 2014], we can generalize this local Lyapunov function of stability
160 to a global Lyapunov function that plays the role of a potential function of any
161 dynamical system. This follows by generalizing condition (a) to allow for saddle points:

$$\nabla L(x^*) = 0, \quad (4)$$

162 Following [Yuan et al., 2014] we show how a Lyapunov function is equivalent to a
163 potential function, when characterizing the stability of a dynamical system. In physics,
164 a potential function ψ can be constructed to describe the flow of – or forces acting on –
165 a particle through a potential energy gradient:

$$\mathbf{F}_{\text{pot}} = \nabla\psi. \quad (5)$$

166 These forces are conservative, where the total work done on the particle is
167 independent of its trajectory (e.g., Gravitational force). However, there are also
168 dissipative, or non-conservative forces, for which the total work done depends on the
169 particle's trajectory and is hence irreversible (e.g., frictional force). At steady-state,
170 these components balance each other, so that the total Force \mathbf{F}_{tot} is zero:

$$\mathbf{F}_{\text{tot}} = \mathbf{F}_{\text{con}} + \mathbf{F}_{\text{dis}} = 0, \quad (6)$$

171 where \mathbf{F}_{con} and \mathbf{F}_{dis} are the conservative and dissipative forces respectively. For
172 example, in electromagnetics, the Lorentz force describes the forces acting on a moving
173 charged particle:

$$\mathbf{F}_{\text{Lorentz}} = q\mathbf{E} + e\mathbf{v} \times \mathbf{B}, \quad (7)$$

174 where q is its charge, \mathbf{v} the velocity of the particle, and \mathbf{E} and \mathbf{B} are the electric and
 175 magnetic forces, respectively. We can therefore write \mathbf{F}_{con} as a combination of Lorentz
 176 force and potential energy induced force:

$$\mathbf{F}_{con} = -\nabla\psi(x) + e\mathbf{v} \times \mathbf{B}, \quad (8)$$

177 while the dissipative force can be expressed as a frictional force (due to dissipative
 178 random fluctuations):

$$\mathbf{F}_{dis} = -S\mathbf{v}. \quad (9)$$

179 Here, S is a symmetric and semi-positive definite friction tensor.

180 Combining these definitions, we can express the total force as a balance of the forces
 181 as defined above, resulting in:

$$S\mathbf{v} + e\mathbf{v} \times \mathbf{B} = -\nabla\psi(x), \quad (10)$$

182 One can generalize this equation for arbitrary n -dimensional systems by replacing
 183 the vector-valued cross product $\mathbf{v} \times \mathbf{B} = T\mathbf{v}$, where T is an antisymmetric matrix to
 184 give the canonical form of (11):

$$(S + T)\mathbf{v} = -\nabla\psi(x), \quad (11)$$

185 Finally, following [Yuan et al., 2014] we can transform this expression into a standard
 186 form using a diffusion tensor Γ (defined as half the covariance of the dissipative random
 187 fluctuations) and a tensor Q (describing friction) satisfying $\nabla \cdot Q\nabla\psi(x) = 0$, by setting
 188 $\psi(x)$ as the Lyapunov function $L(x)$ as defined above so that we get:

$$f(x) = \mathbf{v} = (Q - \Gamma)\nabla\psi(x), \quad (12)$$

189 where $f(x)$ describes the flow of states. This equation describes the evolution or flow
 190 of states resulting from (conservative and dissipative) forces at non-equilibrium
 191 steady-state.

192 In summary, for any dynamical system at non-equilibrium steady-state, we can
 193 express the flow in terms of a scalar potential or Lyapunov function $\psi(x) = L(x)$,
 194 where the flow can always be decomposed into a gradient flow, which minimizes the
 195 potential, and a solenoidal component, that flows on the iso-contours of the potential.
 196 The final move is to associate the Lyapunov function or potential with variational free
 197 energy as follows.

198 3.2 Variational Free Energy

199 Variational free energy is a function of internal states that allows one to associate
 200 the Lyapunov function from (17) with Bayesian model evidence and hence characterize
 201 systemic dynamics in terms of Bayesian inference and the implicit generative models.
 202 This device works by unpacking the non-equilibrium steady-state flow of external,
 203 internal and blanket states. Under this partition, instead of minimizing the Lyapunov
 204 function or (thermodynamic) potential, the internal and active states come to minimize
 205 variational free energy. Crucially, the variational free energy is defined in terms of a
 206 generative model and implicit posterior beliefs encoded by internal states. This
 207 minimization licenses an interpretation of self-organization in terms of belief updating
 208 according to Bayes rules above. In turn, this allows us to specify the resulting
 209 non-equilibrium steady-state in terms of a generative model – and ensuing inference – as
 210 we will see below. First, we will revisit the standard form for dynamics above, in the
 211 setting of generalized coordinates of motion and density dynamics as described by the
 212 Fokker Planck equation.

213 **3.2.1 Generalized Flow**

214 We can describe dynamics in generalized coordinates of motion, denoted with a tilde,
 215 where \tilde{x} is defined as:

$$\tilde{x} = (x, \dot{x}, \ddot{x}, \dots), \quad (13)$$

216 This augments a state with its velocity, acceleration and so on. Later, we will use
 217 generalized coordinates of motion to parameterize a posterior density over (the
 218 generalized motion of) external states (that are hidden behind the Markov blanket).
 219 Among other advantages, generalized coordinates of motion allow one to accommodate
 220 temporal correlations in random fluctuations. Assuming a smooth dynamical system,
 221 subject to random fluctuations, we can describe the motion of states with the Langevin
 222 equation:

$$\dot{\tilde{x}} = f(\tilde{x}) + \tilde{\omega}, \quad (14)$$

223 where $f(\tilde{x})$ is the generalized flow (or time evolution) of states due to forces acting
 224 on the states and $\tilde{\omega}$ are random fluctuations, under the usual Wiener assumptions (the
 225 flow of states is made up of a process of independent, Gaussian increments that follow a
 226 continuous path).

227 In statistical physics the ensuing dynamics is commonly described in terms of
 228 density or ensemble dynamics; namely, the evolution of the probability density $p(\tilde{x})$,
 229 through the Fokker-Planck equation. The Fokker Planck equation can be obtained for
 230 any Langevin equation, using the conservation of probability mass:

$$\dot{p}(\tilde{x}) = \nabla \cdot [\dot{\tilde{x}}p(\tilde{x})] = 0, \quad (15)$$

231 where $\dot{\tilde{x}}p(\tilde{x})$ describes the probability current. This turns the Fokker-Planck
 232 equation into a continuity equation, which reads:

$$\dot{p}(\tilde{x}) = \nabla \cdot \Gamma \nabla p - \nabla \cdot (f(x)p). \quad (16)$$

233 This is a partial differential equation that describes the time evolution of the
 234 probability density $p(\tilde{x})$ under dissipative (first term) and conservative (second term)
 235 forces. At non-equilibrium steady-state, the density dynamics is just the solution to the
 236 Fokker Planck equation:

$$L(\tilde{x}) = -\ln p(\tilde{x}), \quad (17)$$

237 such that $\nabla p = -p \nabla L$ and $\dot{p} = 0$.

238 Using the Helmholtz decomposition from (2), we can now express steady-state flow
 239 in terms of a divergence-free component and a curl-free descent on a scalar Lyapunov
 240 function $L(\tilde{x})$ to obtain

$$f(\tilde{x}) = (Q - \Gamma) \nabla L(\tilde{x}). \quad (18)$$

241 This is the solution at non-equilibrium steady-state and is exactly the same solution
 242 for the flow of particles in the classical treatment above. Crucially, we can now see that
 243 the Lyapunov function is the negative log probability of finding the system in any
 244 (generalized) state $L(\tilde{x}) = -\ln p(\tilde{x})$. This is also known as the self-information of a state
 245 in information theory (also known as surprisal, or more simply surprise). In Bayesian
 246 statistics it is known as the negative log evidence.

247 In summary, any weakly mixing dynamical system that at non-equilibrium
 248 steady-state will evince a flow that can be decomposed into a gradient flow on surprise
 249 and an accompanying solenoidal flow. Because we can associate the Lyapunov function

250 in (18) with a free energy [Seifert, 2012], the system is effectively minimizing a free
251 energy in its convergence to a set of attracting states (known as a random dynamical
252 attractor), which have a high probability of being occupied [Crauel and Flandoli, 1994];
253 namely a high marginal likelihood or evidence. This construction is used extensively in
254 biophysical research fields, such as protein folding to solve for steady-state
255 solutions [Dinner et al., 2000], [Lammert et al., 2012].

256 3.2.2 Least Action Principles

257 Physics offers a useful formalism to understand, at a quantitative level, the ability of
258 biological systems (as evidenced by regulative development and regeneration) to work
259 towards an invariant outcome, despite various perturbations. Understanding this
260 'goal-directed' activity is an important open problem in biological control.

261 The least action principle can predict the emergence of form, in terms of the flow or
262 paths of least action in biological systems. For example, in colonies, ants find the paths
263 of least action to harvest food and bring it to the colony. This example considers their
264 paths as flow channels, or trajectories, finding the least average action for each instance
265 of foraging, given available resources. More generally, minimization of action in an open
266 system leads to structure formation. The 'flows' in such (dissipative) systems are of
267 energy, matter and constituent elements along the paths of least action. An open
268 dynamical system tends towards its state of least action, or the 'most action efficient
269 state'. A canonical example of the emergence of such dissipative structures is when a
270 moving fluid (e.g., a river) erodes obstructions to its flow to form a network of flow
271 channels.

272 In (dissipative) random dynamical systems [Arnold, 1995], [Crauel and Flandoli,
273 1994], action is not minimized for each element of the system, but, on average over an
274 ensemble of elements (or repeated trajectories of the same element) [Georgiev and
275 Georgiev, 2002], [Georgiev et al., 2015], [Georgiev and Chatterjee, 2016], [Georgiev
276 et al., 2017]. Obstructive-constraint minimization therefore reduces action for each
277 event within the system and self-organizes it, forming a flow structure that could be
278 construed as a dissipative structure [England, 2015], [Evans and Searles,
279 2002], [Prigogine, 1978]. Crucially, since self-organizing open systems are not
280 conservative, their structured flow is quintessentially dissipative. While the Lyapunov
281 function of a physical system is readily used to establish the stability of a fixed point in
282 dynamical systems, physicists commonly use the Lagrangian to solve the trajectory of a
283 systems states. Classically, for a conservative system, the Lagrangian is defined as:

$$L = T - V, \quad (19)$$

284 where V is the potential energy of the system, defined through the constraints of the
285 system, and T is the kinetic energy of the particles that constitute the system at hand.
286 For any Lagrangian, the trajectory of states in generalized coordinates $(t, \tilde{x}(t), \dot{\tilde{x}}(t))$ are
287 given by the solutions to the the Euler-Lagrange equation, which are bound by the
288 principle of variations to be functions for which the following functional has extrema
289 (i.e., is stationary):

$$S(\tilde{x}) = \int_{t_1}^{t_2} L(t, \tilde{x}(t), \dot{\tilde{x}}(t)) dt. \quad (20)$$

290 S integrates the Lagrangian of generalized states for boundary conditions defined for
291 initial and final time points t_1 and t_2 . The most likely path between these points is
292 obtained when the functional derivative is zero; i.e., $\delta S = 0$. This is the Hamilton's
293 principle. In this case, the equations of motion are derived from the Euler-Lagrange
294 equations which are the solutions of the principle of least action:

$$\frac{d}{dt} \frac{\partial L}{\partial \dot{\tilde{x}}_i} - \frac{\partial L}{\partial \tilde{x}_i} = 0 \quad \text{for } i = 1, 2, \dots, n. \quad (21)$$

Where \tilde{x}_i are the generalized coordinates and $\dot{\tilde{x}}_i$ the generalized velocities.

For dissipative systems, this equation has additional dissipative terms. For example, if the dissipative function depends on the square of the velocity:

$$F = \frac{1}{2} k \dot{\tilde{x}}^2 \quad (22)$$

Then the Euler-Lagrange equations become:

$$\frac{d}{dt} \left(\frac{\partial L}{\partial \dot{\tilde{x}}_i} \right) - \frac{\partial L}{\partial \tilde{x}_i} + \frac{\partial F}{\partial \dot{\tilde{x}}_i} = 0 \quad (23)$$

The constraints to motion of the agents in a system are given additionally by the Lagrange multipliers.

$$\delta \int_{t_1}^{t_2} [L(t, \tilde{x}(t), \dot{\tilde{x}}(t)) + \sum_k \lambda_k(t) g_k(t, \tilde{x}(t))] dt = 0 \quad (24)$$

Where λ_k are the Lagrange multipliers, and g_k are the constraints [Arfken and Weber, 1995]. The solutions are the constrained Lagrangian equations of motion, which with the added dissipative terms are as follows.

$$\frac{d}{dt} \left(\frac{\partial L}{\partial \dot{\tilde{x}}_i} \right) - \frac{\partial L}{\partial \tilde{x}_i} + \frac{\partial F}{\partial \dot{\tilde{x}}_i} = \sum_k \lambda_k \frac{\partial g_k}{\partial \tilde{x}_i} \quad (25)$$

Terms with random noise can also be added to this equation, which are pertinent for biological systems [El Kaabouchi and Wang, 2015]. Because the Lagrangian describes the trajectories of particles under forces, the functional S is the action of the system. Hence, when the variational principle is applied to the action of a system in this manner, it is referred to as a *least action principle*. To apply least action principles to the kind of systems of interest in biology, it is necessary to consider the action of an ensemble of systems of particles. Minimizing the average action allows individual trajectories to deviate from their paths of least paths, so that they can reduce the action of other particles. The most likely solution for an ensemble minimizes the ensemble average of action, compared to other arrangements of particles and implicit constraints on their flow. As the system evolves, it searches forever lower minima of this average action [Georgiev and Georgiev, 2002], [Georgiev et al., 2015], [Georgiev and Chatterjee, 2016], [Georgiev et al., 2017]. This means that the principle of least action does not apply in isolation to each member of the ensemble but is contextualized by coupling between particles that depend upon many characteristics. These characteristics include: the number of particles, the number of interactions, the total action of the system within certain interval of time, *etc.* Furthermore, these interdependent functions (interfunctions) are bound by power law relations [Georgiev et al., 2015], [Georgiev and Chatterjee, 2016], [Georgiev et al., 2017]. From our perspective, the key observation here is that any (dissipative) random dynamical system can be formulated as a gradient flow on the log likelihood of its states. This is reflected in our solution $L(\tilde{x}) = -\ln p(\tilde{x})$ to the Fokker-Planck equation in (17), which means the action is the time or path integral of the marginal likelihood or self-information:

$$S = \int_{t_1}^{t_2} L(\tilde{x}(t)) dt = \int_{t_1}^{t_2} \ln p(\tilde{x}|m) dt, \quad (26)$$

327 for any system or model m . This means, the least action integral over the Lagrangian
328 turns into an integration over the self-information of states, which is known as entropy
329 in information theory. In short, the principle of least action manifests as a principle of
330 least entropy – for systems that possess a random dynamical attractor – and thereby
331 obtain non-equilibrium steady-state. We now consider the specific structure of the
332 system or model m that underwrites Bayesian inference; namely, the Markov blanket.

333 3.2.3 Markov Blanket

334 A robust literature is developing around the ability of cells and many other aneural
335 systems measuring aspects of their environment via specific sensors [Baluška and Levin,
336 2016]. All biological systems can be analyzed in terms of sensory and internal states and
337 the relationships between them [Rosen, 2012].

338 A Markov partition separates all states $x \in X$ into external $e \in E$, sensory $s \in S$,
339 active $a \in A$, and internal states $i \in I$ (with their generalized versions \tilde{x} , \tilde{e} , \tilde{s} , \tilde{a} , and \tilde{i}),
340 so that

$$\tilde{x} \in X = E \times S \times A \times I, \quad (27)$$

341 where \times denotes the Cartesian product that returns a product set of sets. The
342 ensuing partition is defined in table 1. The Markov blanket separating external and
343 internal states is hence given by $S \times A$, as depicted in Figure 1. The partition into
344 external, internal and blanket states rests upon conditional independencies implicit in
345 the system’s equations of motion or dynamics. In brief, external and internal states
346 depend only upon blanket states, subject to the constraint that sensory states are not
347 influenced by internal states and active states are not influenced by external states.

348 With the Markov partition (and associated influences) in hand, the flow $f(\tilde{x})$ can
349 then be decomposed into 4 parts:

$$\begin{aligned} & f_e(\tilde{e}, \tilde{s}, \tilde{a}) \\ & f_s(\tilde{e}, \tilde{s}, \tilde{a}) \\ & f_a(\tilde{s}, \tilde{a}, \tilde{i}) \\ & f_i(\tilde{s}, \tilde{a}, \tilde{i}) \end{aligned} \quad (28)$$

350 The response of active and internal states, to sensory stimuli, therefore, becomes

$$\begin{aligned} (a) \quad & f_a(\tilde{s}, \tilde{a}, \tilde{i}) = (Q_a - \Gamma_a) \nabla_{\tilde{a}} L(\tilde{s}, \tilde{a}, \tilde{i}) \\ (b) \quad & f_i(\tilde{s}, \tilde{a}, \tilde{i}) = (Q_i - \Gamma_i) \nabla_{\tilde{i}} L(\tilde{s}, \tilde{a}, \tilde{i}) \\ (c) \quad & L(\tilde{s}, \tilde{a}, \tilde{i}) = -\ln p(\tilde{s}, \tilde{a}, \tilde{i} | m), \end{aligned} \quad (29)$$

351 where m describes the Markov partition that defines the underlying random
352 dynamical system (e.g., a cell).

Set	Dependent sets	Description of set contents
sample space Ω		random fluctuations or outcomes
external states E	$E \times A \times \Omega$	hidden states causing sensory inputs.
sensory states S	$E \times A \times \Omega$	signals mapping from external to internal states.
active states A	$S \times I \times \Omega$	action determined by sensory and internal states.
internal states I	$I \times S \times \Omega$	internal states causing action.

Table 1. Table denoting variables of Bayesian Inference.

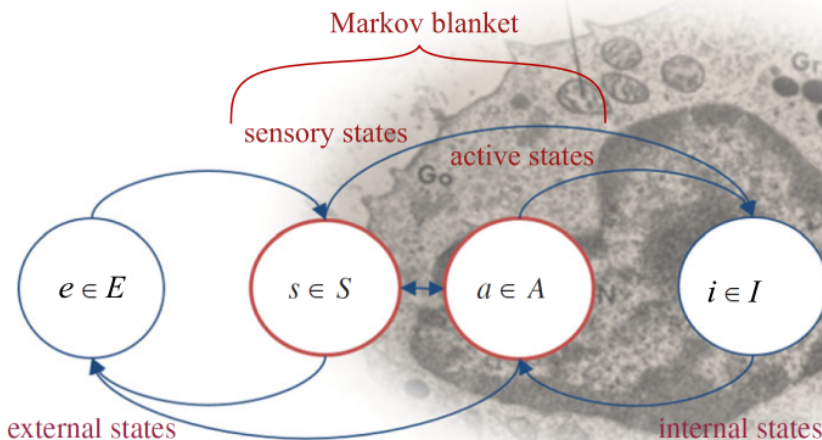


Fig 1. Markov blanket schematic. The internal and external states of each cell are separated by a Markov blanket, which comprises the cell’s sensory and active states. The internal states can be interpreted as the intracellular states of a cell, such as its gene expression levels. While the sensory states correspond to the surface states of the cell membrane, such as receptors and ion channel states. The active states are given by the underlying active components of the cytoskeleton, such as actin filaments and microtubules. By associating the gradient flows of the Markov blanket partition with Bayesian belief updating, self-organization of internal states – in response to sensory fluctuations – can be thought of as perception, while active states couple internal states back to hidden external states vicariously, to provide a mathematical formulation of action and behavior. Adapted from [Friston et al., 2015].

353 Inserting (c) into (a) and (b), gives:

$$\begin{aligned}
 (a') \quad f_a(\tilde{s}, \tilde{a}, \tilde{i}) &= (\Gamma_a - Q_a) \nabla_{\tilde{a}} \ln p(\tilde{s}, \tilde{a}, \tilde{i} | m) \\
 (b') \quad f_i(\tilde{s}, \tilde{a}, \tilde{i}) &= (\Gamma_i - Q_i) \nabla_{\tilde{i}} \ln p(\tilde{s}, \tilde{a}, \tilde{i} | m)
 \end{aligned}
 \tag{30}$$

354 The key aspect of this dynamics is that the autonomous (i.e., active and internal)
 355 states of an agent depend upon same quantity, which reduces to the log probability of
 356 finding the agent in a particular state; where the agent’s states comprise the internal
 357 states and their Markov blanket. In this partition, autonomous states are those states
 358 that do not depend upon external states; namely, internal and active states. Solving
 359 equation (30) for the evolution f of active and internal states thus corresponds to
 360 evaluating the gradients of the log probabilities above that correspond to the
 361 Lagrangian of an open system. In general, this would be a very difficult problem to
 362 solve; however, we can now replace the Lagrangian with a variational free energy
 363 functional of a probabilistic model of how a system thinks it should behave, as follows.

364 3.2.4 Kullback-Leibler Divergence and Variational Free Energy

365 Using the above Markov blanket partition, we can now interpret internal states as
 366 parametrizing some arbitrary probability density $q(\tilde{e})$ over external states. This allows
 367 us to express the Lagrangian or Lyapunov function as a free energy functional of beliefs,
 368 and implicitly a function of the internal states. In probability theory, an ergodic random

369 dynamical system is a system which has the same behavior averaged over time as
 370 averaged over the system's states. In physics ergodicity implies that a system satisfies
 371 the ergodic hypothesis of thermodynamics, which says that over a sufficiently long time
 372 span, the time spent by a system in some region of state or phase space of individual
 373 states (with the same energy) is proportional the probability of the system be found in
 374 that region [Boltzmann, 2009].

375 Using the statistical definition for an expected value as averaged over all states
 376 $x \in \mathbf{R}$,

$$E[X] = \int_{\mathbf{R}} xp(x) dx, \quad (31)$$

377 we can then express the variational free energy through the introduction of the
 378 Kullback-Leibler Divergence:

$$D_{\text{KL}}(p||q) = \int_{-\infty}^{\infty} p(x) \ln \frac{p(x)}{q(x)} dx, \quad (32)$$

379 which is the expectation of the logarithmic difference between the probabilities p
 380 and q , where the expectation is taken using the probabilities p .

381 Therefore, in place of the log density $\ln p(\tilde{s}, \tilde{a}, \tilde{i}|m)$ above, we can now write a
 382 variational free energy F that corresponds to the logarithmic difference between the
 383 (variational) density or Bayesian beliefs about external states $q(\tilde{e})$ and actual
 384 probability densities $p(\tilde{e}, \tilde{s}, \tilde{a}, \tilde{i}|m)$ of all states under the Markov blanket m defined in
 385 Table 1 and Figure 1:

$$\begin{aligned} F(\tilde{s}, \tilde{a}, \tilde{i}) &= \int_{\tilde{e}} q(\tilde{e}) \ln \frac{q(\tilde{e})}{p(\tilde{e}, \tilde{s}, \tilde{a}, \tilde{i}|m)} d\tilde{e} \\ &= -\ln p(\tilde{s}, \tilde{a}, \tilde{i}|m) + D_{\text{KL}}(q(\tilde{e})||p(\tilde{e}|\tilde{s}, \tilde{a}, \tilde{i})). \end{aligned} \quad (33)$$

386 The first term is also called (Bayesian negative log) model evidence, or marginal
 387 likelihood, which essentially describes the likelihood that the sensory inputs were
 388 generated by a generative model implicit in the Markov blanket m . The second term is
 389 referred to as relative entropy and works as to minimize the divergence between the
 390 variational and posterior density $q(\tilde{e})$ and $p(\tilde{e}|\tilde{s}, \tilde{a}, \tilde{i})$ respectively. As a result,
 391 maximizing model evidence results into minimizing the free energy of the system, and
 392 because the divergence of the second term can never be less than zero, free energy is an
 393 upper bound on the negative log evidence. Using this expression, the flow of
 394 autonomous (i.e., active and internal) states becomes

$$\begin{aligned} (a'') \quad f_a(\tilde{s}, \tilde{a}, \tilde{i}) &= (Q_a - \Gamma_a) \nabla_{\tilde{a}} F(\tilde{s}, \tilde{a}, \tilde{i}) \\ &= (\Gamma_a - Q_a) \nabla_{\tilde{a}} \ln p(\tilde{s}, \tilde{a}, \tilde{i}|m) - (\Gamma_a - Q_a) \nabla_{\tilde{a}} D_{\text{KL}} \\ (b'') \quad f_i(\tilde{s}, \tilde{a}, \tilde{i}) &= (Q_i - \Gamma_i) \nabla_{\tilde{i}} F(\tilde{s}, \tilde{a}, \tilde{i}) \\ &= (\Gamma_i - Q_i) \nabla_{\tilde{i}} \ln p(\tilde{s}, \tilde{a}, \tilde{i}|m) - (\Gamma_i - Q_i) \nabla_{\tilde{i}} D_{\text{KL}}. \end{aligned} \quad (34)$$

395 The key thing to note here is that the gradient descent on variational free energy
 396 will reduce the divergence in equation (32) to its lower bound of zero (because the
 397 divergence cannot be less than zero). At this point, the gradients of the divergence in
 398 equation (34) disappear and the dynamics reduce to the self-organization in equation
 399 (30), which is what we want to solve.

400 This is important because the variational free energy bound in equation (33) can be
 401 evaluated in a straightforward way given a generative model; namely, the joint

402 probability over (generalized) external, internal and blanket states. On this view, we
403 can associate the joint probability in equation (33) with a likelihood; namely, the
404 probability of a cell’s states, given external states and a prior; namely, the prior
405 probability of a cell’s states (i.e., internal states and their Markov blanket). Finally, this
406 means that $q(\bar{\epsilon})$ plays the role of a posterior density over hidden or external states
407 under a particular Markov blanket or model (m). Crucially, this variational posterior is
408 parameterized by internal states. In other words, we can talk about the internal states
409 encoding beliefs about external states.

410 In summary, to solve the problem of self-organization, we can specify a generative
411 model for a cell and integrate (34). Before we turn to the construction of this generative
412 model, we will briefly consider the ensuing (Bayesian filtering) scheme we used below to
413 simulate self-organization in terms of dynamical belief updating in subsequent sections.

414 3.3 Bayesian Filtering and Self-Organization

415 We have seen above that one can replace the Lyapunov or Lagrangian function for
416 any dynamics of a system that is equipped with a Markov blanket with a variational
417 free energy that depends upon a generative model. This variational free energy is,
418 effectively, a variational (upper) bound on model evidence; here, interpreted in terms of
419 the probability of an agent’s state (see equation (1)). This means that one can always
420 interpret any self-organization to non-equilibrium steady-state (i.e., no time variation of
421 the density over states) in terms of maximizing a quantity that plays the role of
422 Bayesian model evidence. This is sometimes referred to as self-evidencing, a concept
423 from brain sciences, where the agent (usually the brain) has to identify an evidentiary
424 boundary between itself and its environment as a necessary condition for
425 inference [Hohwy, 2016], [Moutoussis et al., 2014].

426 The variational free energy here is exactly the same mathematical construct used in
427 statistics and variational Bayes. Simple examples of this include Kalman filtering and
428 particle filtering, for inferring hidden states under dynamic Bayesian networks. Similar
429 schemes have been used to infer genetic regulatory network structures from available
430 genomic microarray time-series measurements [Lijun et al., 2008], [Noor et al., 2012].
431 The generalization of methods like Kalman filtering to a non-linear setting (in
432 generalized coordinates of motion) leads to generalized (variational) filtering. These
433 induce a variational free energy bound on model evidence by assuming under a
434 fixed-form (usually a Gaussian) for the variational density $q(\bar{\epsilon})$ above. This fixed form
435 assumption underwrites the variational approximation that renders an intractable
436 integration problem (30) into a tractable optimization problem that can be expressed as
437 a gradient descent (34). The ensuing optimization rests upon a particular generative
438 model – and implicit priors – which, in the research presented in this paper corresponds
439 to the target morphology, or goal state [Friston et al., 2008], [Friston, 2008].

440 In summary, variational filtering is the quantification and minimization of a
441 variational free energy, which places an upper bound on the dispersion of a particle’s
442 internal states and their Markov blanket [Buckley et al., 2017], [Friston et al., 2010].
443 Variational free energy hence converts any process of self-organization into a gradient
444 descent on a free energy landscape, where basins correspond to attractor states, or goal
445 states – akin to the target morphology – as described next.

446 4 Modeling Morphogenesis

447 In this section, we illustrate self organization to non-equilibrium steady-state using
448 the variational principles described above, by trying to explain the behavior of a model
449 of pattern regulation by considerations of information processing and error minimization

450 with respect to a specific target morphology. In this setting, the game changes subtly
451 but profoundly. Above, we have seen that the dynamics of any random dynamical
452 system, equipped with a Markov blanket, can be formulated in terms of a gradient flow
453 on variational free energy. As a reminder, a Markov partition separates all states $x \in X$
454 into external $e \in E$, sensory $s \in S$, active $a \in A$, and internal states $i \in I$ (with their
455 generalized versions \tilde{x} , \tilde{e} , \tilde{s} , \tilde{a} , and \tilde{i}). Variational free energy rests on an unknown
456 generative model that produces the dynamics responsible for self-organization. Here, we
457 turn this formulation on its head by specifying a generative model – and implicit
458 variational free energy function – and simulate self-organization by solving the equations
459 of motion in equation (34). In other words, we specify the form of the attracting set in
460 terms of a probabilistic generative model of how external states perturb blanket states
461 (i.e., a likelihood model) and how external states evolve (i.e., a prior). To do this, we
462 have to simulate both the flow of autonomous (i.e., internal and active) states of each
463 cell or agent and the external states that constitute its immediate milieu. In other
464 words, we have to specify the external dynamics as a generative process and a
465 generative model of that process entailed by the flow of internal states.

466 To illustrate the basic phenomenology, we will consider the self-assembly of an
467 ensemble of cells to simulate morphogenesis, under different conditions. The generative
468 model required is relatively simple but serves to illustrate the potential utility of this
469 variational (free energy) formulation of self-assembling autopoietic behavior.

470 4.1 Constructing the Model

471 We need to specify the generative model given by the probability density $p(\tilde{s}, \tilde{a}, \tilde{i}|m)$
472 of sensory states s , active states a and internal states i , as well as the dynamics of the
473 environment, determined through the flow $f_{\tilde{e}}$ and $f_{\tilde{s}}$ of external states e and sensory
474 states s , respectively. This allows us to specify the requisite equations of motion for the
475 system and its external states. Here, we will adopt a probabilistic nonlinear mapping
476 with additive noise:

$$\begin{aligned} s &= g^{(1)}(e^{(1)}) + \omega^{(1)} \\ e^{(1)} &= g^{(2)}(e^{(2)}) + \omega^{(2)}, \end{aligned} \quad (35)$$

477 where the superscripts denote the first and second levels of our hierarchical model g .
478 Gaussian assumptions about the random fluctuations or noise ω mean that we can write
479 the requisite likelihood and priors as:

$$\begin{aligned} p(\tilde{s}, \tilde{a}, \tilde{i}|\tilde{e}^1) &= \mathcal{N}(g^{(1)}(e^{(1)}), \Pi^{(1)}) \\ p(\tilde{e}^1|\tilde{e}^2) &= \mathcal{N}(g^{(2)}(e^{(2)}), \Pi^{(2)}). \end{aligned} \quad (36)$$

480 where \mathcal{N} is the normal distribution, and $\Pi^{(t)}$ denotes the precision (or inverse
481 variance) of the random fluctuations.

482 We then construct the approximate posterior density $q(\tilde{e})$ introduced in (32) using
483 the associated Lagrangian or Lyapunov function

$$\begin{aligned} L(\tilde{x}) &= -\ln p(\tilde{s}, \tilde{a}, \tilde{i}, \tilde{e}|m) \\ &= -\ln p(\tilde{s}, \tilde{a}, \tilde{i}|\tilde{e}^1) - \ln p(\tilde{e}^1|\tilde{e}^2), \end{aligned} \quad (37)$$

484 Under a Laplace assumption, the variational density becomes a normal distribution:

$$q(\tilde{e}) = \mathcal{N}(\tilde{i}, -\nabla_{\tilde{i}\tilde{i}} L(\tilde{s}, \tilde{a}, \tilde{i}, \tilde{i})), \quad (38)$$

485 where $\nabla_{\tilde{i}} L(\tilde{s}, \tilde{a}, \tilde{i})$ denotes the curvature of the Lagrangian with respect to
 486 internal states. With this generative model and assumed form for the variational
 487 density, we can now evaluate the variational free energy for any given sensory state and
 488 perform a gradient descent according to equation (34).

489 An interesting technical detail here rests upon the use of generalized coordinates of
 490 motion. This means that one can associate the dissipative flow with a gradient descent
 491 on the expected energy function in equation (37) (noting that the entropy term of the
 492 variational free energy does not depend upon the means encoded by internal states).
 493 Furthermore, we can associate the divergence-free flow with an update term, so that

$$\begin{aligned}
 \Gamma \nabla F(\tilde{s}, \tilde{a}, \tilde{i}) &= \nabla E_q[L(\tilde{s}, \tilde{a}, \tilde{i})] \\
 Q_i \nabla F(\tilde{s}, \tilde{a}, \tilde{i}) &= D\tilde{i} = (i^t, i, \dots) \\
 \nabla \cdot D\tilde{i} &= 0.
 \end{aligned}
 \tag{39}$$

494 Here, D is a block matrix operator that acts upon generalized coordinates of motion
 495 to return generalized motion (with zero divergence). Γ and Q are the diffusion and
 496 friction tensor introduced previously, and $E_q[L]$ is the expected value of L under the
 497 variational density; i.e., posterior belief $q(\tilde{e})$. This divergence free component effectively
 498 plays the role of an update term in Bayesian filtering – that can be interpreted as a
 499 gradient descent on variational free energy in a moving frame of reference. See [Friston
 500 et al., 2010] for details. In summary, this scheme can be regarded as a generalized
 501 (variational) filter, in which the internal states become the expected values of the
 502 external (hidden) states.

503 Finally, we assume that action is sufficiently fast to use the adiabatic approximation
 504 $\tilde{e} \approx \tilde{a}$, which greatly simplifies the specification of external dynamics.

505 4.2 Variational Free Energy Minimization

506 By effectively minimizing variational free energy, each Markov blanket or agent will
 507 appear to engage in belief updating, under the generative model, so that the evolution
 508 of the system will inevitably lead to a non-equilibrium steady state of minimal free
 509 energy. This provides a rigorous foundation for an intuitive concept familiar to all
 510 students of development and regeneration: cells act, remodeling tissues and organs, to
 511 minimize the global difference between the current configuration and a species-specific
 512 anatomical goal state [Pezzulo and Levin, 2015], [Pezzulo and Levin, 2016]. Cells and
 513 cell groups change their behavior based on signals they perceive from their environment
 514 (measurement) and act with respect to expectations (genetically encoded, and shaped
 515 by cellular learning) [Baluška and Levin, 2016].

516 Because free energy corresponds to (an upper bound on) Bayesian model evidence
 517 $-\ln p(\tilde{s}, \tilde{a}, \tilde{i}|m)$ as introduced in equation (33), this self-organizing behavior will also
 518 appear to be self-evidencing. This description of dynamics uses terms like Bayesian
 519 beliefs $q(\tilde{e})$ and self-evidencing in a purely technical (non-propositional) sense, which
 520 can be ascribed to simple systems like macromolecules and cells. The simulations below
 521 consider a small set of cells that are equipped with the same generative model such that
 522 they collectively self-organize to minimize variational free energy in an interdependent
 523 way, which has all the hallmarks of morphogenesis. This example is appropriate to
 524 models such as the highly-regenerative planaria [Levin et al., 2019], [Durant et al., 2016].

525 All the cells in the simulation start off with random initial signaling profiles near the
 526 center of their environment. In order for them to self-organize to the target
 527 configuration, each cell must infer its own location in the ensemble by forming and
 528 testing beliefs (or predictions) $q(e)$ about the hidden causes of the signaling
 529 concentrations it senses (i.e., , the secretion profiles and hence cell identities of the other

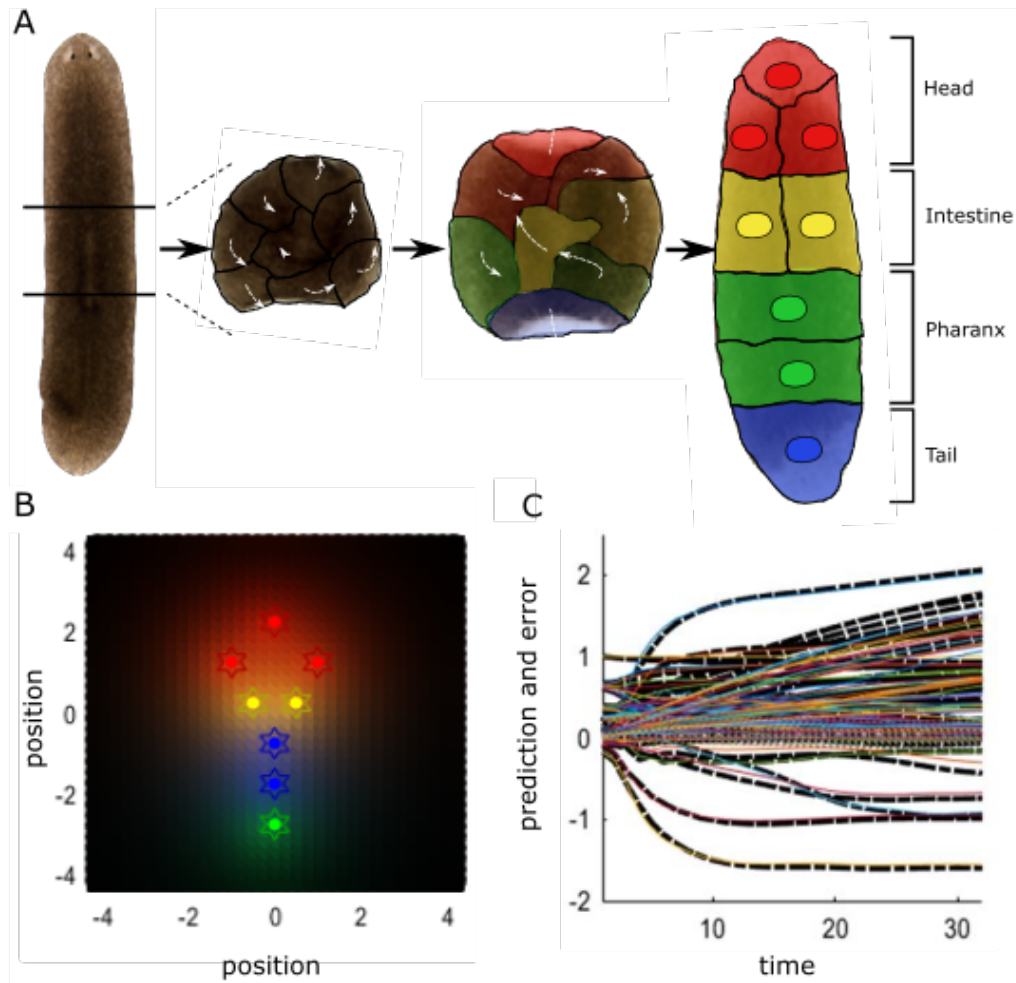


Fig 2. Schematic of variational Bayesian simulation of morphogenesis illustrated via a type of regenerative patterning observed in planarian flatworms and other organisms. **A:** When dissecting out the center piece of a planarian flatworm, the constituent cells will remodel into a new worm. Here, cells that form different tissue types were grouped together as one cell in the simulation for simplicity, with the cell signaling types defined in Figure 3. **B:** Expected Signal concentrations (background color) at each final position (colored stars) in the target morphology encodes the cellular model of inference, with the color coding from **A**. **C:** Cells are constantly comparing their sensed signal concentrations to their expectations by minimizing their free energy functional, which effectively aims to reduce the prediction error $\tilde{\epsilon}$ defined in equation (47) (dashed lines) on expected sensory states s defined in equation (40) (continuous lines).

530 cells (Figure 2). This can be formalized in terms of minimizing free energy, which
 531 effectively minimizes prediction errors $\tilde{\epsilon}$.

532 In more detail, in these simulations, each cell has control over what level of signals it
 533 can secrete of the four different generic types used here, and each cell can move in any
 534 direction. Furthermore, each cell has a generic place-encoded model of some (shared)
 535 target configuration based on signaling concentrations that would be sensed under that
 536 configuration. This means that for each of the four possible cell types associated with
 537 specific positions in the cell cluster cells expect to sense specific concentrations of

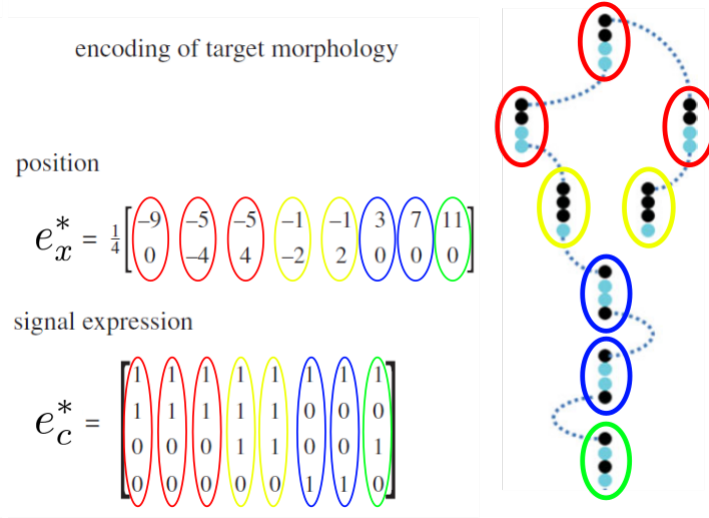


Fig 3. Encoding of Target morphology. This modeling scheme casts the arrangement of cells as an inference process, where the target morphology is encoded in each cell by expectations of external signals e_c^* for any given position e_x^* in the defined target morphology that constitutes the final configuration of cells. Each row in e_c^* corresponds to a different signaling type, while every column represents the signal expression states for a different cell. This figure uses the same color coding used to differentiate cell types as in Figure 2.

538 signaling molecules. See Figure 3.

539 Sensory states s corresponded to chemotactic concentrations of intracellular,
 540 exogenous and extracellular signals, such that:

$$s = \begin{bmatrix} s_c \\ s_x \\ s_\lambda \end{bmatrix} = \begin{bmatrix} e_c \\ e_x \\ \lambda(e_x, e_c) \end{bmatrix} + \omega, \quad (40)$$

541 where e are the external states of concentrations c and positions x of other cells.

542 The signal concentration s_λ at each position of the i -th cell is given through the
 543 secretion and diffusion of signaling molecules of each other cell j and itself, given by the
 544 coefficient:

$$\lambda_i(e_x, e_c) = \tau \cdot \sum_j e_{cj} \cdot \exp(-k d_{ij}), \quad (41)$$

545 where e_{cj} is the combination of the four signals expressed at each position j ,
 546 depicted in Figure 2B as colored coded around the target positions e^* , which are
 547 defined in Figure 3, and

$$d_{ij} = |e_{xi} - e_{xj}|, \quad (42)$$

548 is the distance between the i -th cell and the remaining cells, to which the secreted
 549 signal diffuses with diffusion coefficient k .

550 To preclude over-sensitivity to concentration gradients in early simulation steps –
 551 and model the emergence of cellular response to extracellular signals (e.g., through
 552 increased expression of cell surface receptors over time) – a time sensitivity factor
 553 $\tau \in [0, 1]$ was included, with

$$\tau = 1 - \exp\left(-\frac{t}{T}\right), \quad (43)$$

554 where $T = \frac{1}{\ln(2)}$, analogous to the half-life in exponential decay. This can be thought
 555 of as modeling changes in interfunctions that describe the characteristics of systems,
 556 which we introduced in section 3.2.2.

557 By analogy to stem cell-like behavior, we specify the same generative model g for
 558 each cell:

$$g(e) = \begin{bmatrix} e_c^* \\ e_x^* \\ \lambda^* \end{bmatrix} \sigma(e), \quad (44)$$

559 where $\lambda^* = \lambda(e_c^*, e_x^*)$ is the signal concentration at the target locations, and

$$\sigma(e_j) = \frac{\exp e_j}{\sum_j \exp e_j} \quad (45)$$

560 is the softmax function (or normalized exponential). This function is often used in
 561 neural networks to enforces a sum to one constraint, which allows an interpretation as a
 562 categorical distribution over mutually exclusive outcomes.

563 Using these expressions – and the equations of motion from the previous sections –
 564 we can express the flow of internal and active (*i.a.* autonomous) states from (34) as

$$\begin{aligned} (a'') \quad f_a(\tilde{s}, \tilde{a}, \tilde{i}) &= (Q_a - \Gamma_a) \nabla_{\tilde{a}} F(\tilde{s}, \tilde{a}, \tilde{i}) = D\tilde{a} - \nabla_{\tilde{a}} \tilde{s} \cdot \Pi^{(1)} \tilde{\epsilon} \\ (b'') \quad f_i(\tilde{s}, \tilde{a}, \tilde{i}) &= (Q_i - \Gamma_i) \nabla_{\tilde{i}} F(\tilde{s}, \tilde{a}, \tilde{i}) = D\tilde{i} - \nabla_{\tilde{a}} \tilde{\epsilon} \cdot \Pi^{(1)} \tilde{\epsilon} - \Pi^{(2)} \tilde{i}, \end{aligned} \quad (46)$$

565 while suppressing higher order terms (under the assumption of a smooth system,
 566 which is guaranteed by (43)). Here, $\epsilon = s - g(i)$ is the prediction error associated with
 567 sensory states – the state of chemotactic signal receptors – and can hence be expressed
 568 as:

$$\epsilon = \begin{bmatrix} \epsilon_c \\ \epsilon_x \\ \epsilon_\lambda \end{bmatrix} = \begin{bmatrix} s_c - e_c^* \sigma(i) \\ s_x - e_x^* \sigma(i) \\ s_\lambda - \lambda^* \sigma(i) \end{bmatrix}. \quad (47)$$

569 D corresponds to the matrix derivative operator on generalized states and the signal
 570 precision $\Pi^{(1)}$ is set to 1. We assumed Gaussian priors (with a mean of 0) over the
 571 hidden states with a small precision $\Pi^{(2)}$ (*i.e.*, high variance) with a log precision of
 572 minus two.

573 In summary, under this sort of generative model (with continuous states and
 574 additive Gaussian noise), the internal states organize themselves to minimize
 575 (precision-weighted) prediction error based upon predictions of sensed signaling states
 576 from neighboring cells. In neurobiology, this scheme is also known as predictive coding
 577 and can be regarded as a generalized form of Bayesian filtering as described in section 3.
 578 Predictive coding refers to describing the dynamics of the system in terms of prediction
 579 errors ϵ through accumulation of model evidence $\ln p(\tilde{s}, \tilde{a}, \tilde{i} | m)$, which maximizes
 580 likelihood $p(\tilde{s}, \tilde{a}, \tilde{i} | \tilde{\epsilon}^1)$ [Friston and Kiebel, 2009]. This is the process underlying the
 581 formulation of variational free energy above.

582 In the next section, we describe the results of some numerical analyses that
 583 underwrite the validity of this variational formulation by reproducing empirical
 584 behaviors *in silico*. In particular, we simulate responses of this multicellular ensemble to
 585 perturbations commonly used experimentally.

4.3 Perturbation Simulations

4.3.1 Animal Body Polarity Inversion

First, we introduced a gradient in the generative process for the signaling inputs that each cell receives from its environment, depending on each cell’s chemotactic behavior (sensing and acting upon signals) and signaling outputs (secretion). This represents either a change in the way signaling concentrations are spread, maintained or counterbalanced in the extracellular environment of the cell (reflecting the experimental use of viscosity or osmolarity modifying compounds for example), or in sensitivity of the cell to changes in its environment (similar to the way we use the time sensitivity factor τ). This manipulation could be implemented experimentally by using receptor activity modifying drugs; for example, ethanol for neurotransmitters in the brain, [Banerjee, 2014], or retinoic acid through cross-modulation of cell-surface receptor signaling pathways. [Chambon, 1996].

To simulate formal changes – such as body polarity inversion – one can change the process that generates sensory inputs, as given by (40); namely, the mapping between sensory states s and external states e that constitute chemotactic concentrations of intracellular, exogenous and extracellular signals. Specifically, we changed the mapping $s_x = \tilde{e}_x$ to:

$$\begin{aligned} (a) \quad s_x &= (\tilde{e}_x)^2 \\ (b) \quad s_x &= -(\tilde{e}_x)^2 \end{aligned} \tag{48}$$

for the vertical axis, thereby changing the perceived distance of each cell to another in the vertical direction. In this instance, (a) results in a double head formation, and (b) in a double tail formation (*cf.* Figure 4).

Essentially, by introducing the terms corresponding to the square of the gradients with a different sign in (48), we changed the way sensory states (signaling inputs) were updated from changes in extracellular concentrations (external states) depending on the position of other cells. The squared gradient produces two things:

(1) it causes the signal concentrations to be updated only based on positive (or negative with the minus sign in (48)(b)) values, essentially causing each cell to explain all sensory inputs as an increased signal from one direction.

(2) It increases the sensitivity of sensory inputs to extracellular concentrations (external states), thereby increasing the effective precision.

4.3.2 Anomalous Cell Behavior

Some of the deepest insights into biological regulation come from observing instances where the normally tight processes go awry such as the cellular defection known as cancer [Moore et al., 2017], or disorders of development seen in birth defects. These processes can readily be modeled in our paradigm via changes of cellular decision-making. If we introduce the same type of gradient as in the previous simulations, but for only one cell, then we are effectively altering the sensitivity of that cell to changes in its environment (*cf.* Figure 5).

This can be specified formally as

$$s_{x,j} = (\tilde{e}_{x,j})^2 \text{ for } j = j_f \text{ and } s_{x,j} = \tilde{e}_{x,j} \text{ for } j \neq j_f, \tag{49}$$

where j_f denotes the affected cell.

By introducing a local increase in a cellular signaling, this phenotype can be rescued enabling other cells to respond more definitively to their joint signaling. For example, the induced mutant phenotype above can be rescued by applying a square root to the

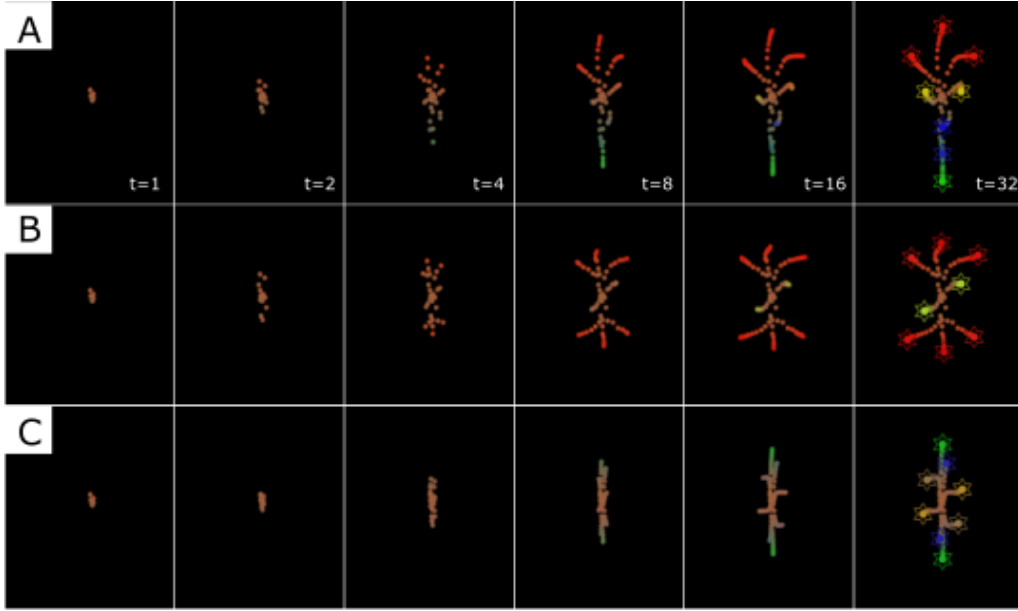


Fig 4. Time-lapse movie montage of simulations of morphogenesis with mirrored anterior/posterior polarity (head and tail positioning). **A:** 8 cells with initially unspecified cell types start to infer a correct target morphology by performing chemotaxis and updating their posterior beliefs, or predictions, q – and hence secretion profile. **B:** Using (48)(a), we introduced a positive squared gradient in the generative process for the signaling inputs that each cell receives from its environment, resulting in double head formation. **C:** Using (48)(b), we introduced a negative squared gradient in the generative process for the sensory inputs that each cell receives from its environment, resulting in double tail formation.

629 distance exponent in the signal concentration of the misbehaving cell. This attenuates
 630 the diffusion of signals given by λ in (41) for the affected cell j_f into:

$$\lambda_{j_f} = \tau \cdot \sum_l e_{cl} \cdot \exp(-k \sqrt{d_{jfl}}). \quad (50)$$

631 In short, with a simple manipulation of extracellular diffusion one can reinstate
 632 normal pattern formation. These examples illustrate how simple changes to
 633 extracellular signaling can have a profound effect on self-organization – an effect that
 634 depends sensitively on the ensemble behavior of cells – that depends upon a shared
 635 generative model. A key point – made by these kinds of simulations – is that one can
 636 reproduce aberrant morphogenesis (and an elemental form of cancer) without changing
 637 any intracellular mechanisms (i.e., the encoding of an implicit generative model). The
 638 message here is that casting morphogenesis, in terms of an inference process means that
 639 the ability of a cell to model its external milieu depends upon the coherence between
 640 the external generative processes and the model of those processes. Perturbations to
 641 either can result in profound changes in ensemble dynamics. Here, we restricted the
 642 manipulations to the external biophysics; i.e., the generative process. In future work, we
 643 will explore a larger repertoire of manipulations that speak to key empirical phenomena.
 644 Matlab software running these simulations, under different conditions is available from
 645 the author and can be downloaded as part of the academic SPM software from
 646 <https://www.fil.ion.ucl.ac.uk/spm/software/> (accessed via a graphical user interface
 647 invoked with the command `>> DEM`).

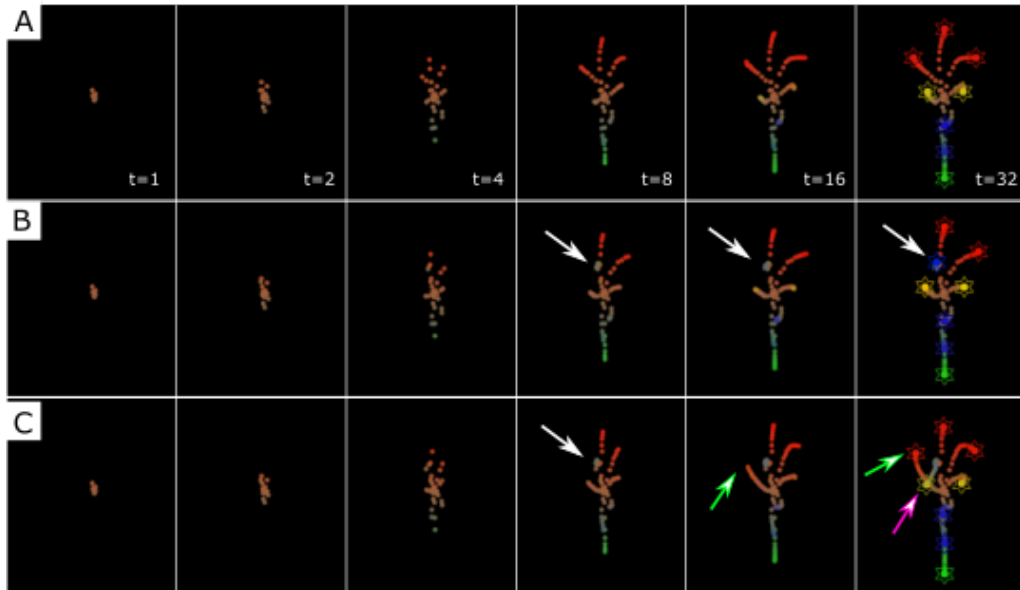


Fig 5. Time-lapse movie montage of simulations of morphogenesis with single cell aberrant signaling. **A:** 8 cells with initially unspecified cell fates start to infer a correct target morphology by performing chemotaxis and updating their beliefs and hence secretion profile. **B:** One of the cells (white arrow) has a perturbed signaling response mechanism and hence fails to correctly infer its place in the ensemble. **C:** The same aberrant cell from B initially is rescued by an increased signaling sensitivity of the other cells, leading another cell (green arrow) to switch position with the aberrant cell (pink arrow).

5 Discussion and Conclusion

Here, we provide a rigorous mathematical foundation for a poorly-understood but very important phenomenon: cellular decision-making, such as occurs during pattern regulation. The Bayesian inference framework enables quantitative models linking sensory mechanisms with functional behaviors in cells and tissues. In section 3 we have shown that the variational free energy that is being minimized in Bayesian inference follows out of classical analytical and statistical physics considerations as a unique form of a least action principle. Specifically, we showed that a Lyapunov function plays the role of a potential function in any dynamical system, and is being minimized to solve the flow of states in that system through a gradient descent. We then introduced the notion of a Markov blanket partition of states that allowed us to replace the Lyapunov function – or the related Lagrangian that is being used to compute the gradient descent in classical least action principles – with a variational free energy functional. This functional turns the classical gradient flow of any dynamical system into a gradient descent on the expectation of the (logarithmic) difference between (Bayesian) beliefs about external states and an actual probability density of all the states – as given by the Kullback-Leibler divergence. For non-equilibrium systems, this transforms an intractable integration problem of a thermodynamic potential into a tractable integration over a probabilistic model of how a system thinks it should behave.

In section 4, we showed how the attractor (or goal) states of the variational free energy landscape – on which the gradient descent described occurs – can be associated with a target morphology in a developmental, regenerative, or aberrant biology setting, thereby casting morphogenesis as an inference process. Through Bayesian inference

671 simulations of such processes, we showed how we can control the morphogenesis
672 outcome through manipulations to the external biophysics (i.e., the generative process
673 of our simulations) through knowledge of the underlying generative model of the
674 inference process.

675 Before discussing these simulation results in more detail and drawing conclusions for
676 the applications of this Bayesian formulation of self-organization to the experimental
677 control of morphogenesis in real biological systems, we will first analyze the the
678 mathematical assumptions that went into this model.

679 5.1 Summary of Mathematical Assumptions Underlying the 680 Model

681 The variational formulation that underlies the simulations above demand a
682 sufficiently smooth system. This means that abrupt changes in signaling can disrupt the
683 simulations. In our applications, this effect was finessed by using a time sensitive
684 coefficient from (43).

685 This type of time dependent sensitivity emerges from theoretical considerations and
686 can, in principle, be tested for empirically in real biological systems. This sort of time
687 sensitivity may manifest either through an increase of receptors, or proteins modifying
688 the efficiency of signal transduction inside the cell; for example, in the levels of
689 G-proteins, which act as molecular switches for multiple signaling pathways [Gilman,
690 1987]. When analyzing a cellular system that starts from a pre-specified configuration,
691 such as in later stages of development or regeneration, this time-sensitivity may not be
692 a prominent feature of the (implicit) generative model.

693 We have also made Gaussian assumptions about the fluctuations ω in the flow of
694 states and a Laplace assumption for the approximate posterior density (*cf.* (38)). The
695 Laplace assumption is often applied to modelling dynamics in neuronal populations, by
696 a Gaussian neuronal population density. This allows population dynamics to be
697 described by equations concerning the evolution of the population's mean and
698 covariance, using the Fokker-Planck equation [Marreiros et al., 2009], [Friston et al.,
699 2007]. This assumption has also been applied to gene regulatory networks [Imoto et al.,
700 2001], which motivate the notion of internal states used in this work.

701 Most fundamentally, we have assumed the existence of a Markov blanket, which
702 separates external and internal states through a set of active and sensory states. This
703 statistical boundary does not necessitate a stationary or unique boundary between
704 agents, but can be mutable [Clark, 2017], and conform to the type of simulations
705 in [Friston, 2013]. Nevertheless, it needs to be verified empirically that signal
706 transmission and adaptive responses on a cellular level are not instantaneous (as in our
707 adiabatic approximations), and that active states indeed cause changes in sensory states.

708 Finally, we have appealed to nonequilibrium steady-state (under ergodic
709 assumptions) for the type of dynamics studied here. While this is a common assumption
710 made in the description of dynamical systems, some argue that any biological system is
711 non-ergodic at a molecular level [Longo and Montévil, 2013]. Yet it remains unclear
712 whether this holds true for states of cellular signaling and genetic expression investigated
713 here. Furthermore, the ergodic (e.g., weakly mixing) assumptions that underlie the free
714 energy principle are only those inherent in the existence of a pullback attractor. The
715 pullback attractor is defined as a state, or set of states, to which a random dynamic
716 system would converge to (yet not necessarily reach due to random fluctuations) if given
717 enough time and with continuous mixing under these ergodic assumptions. In other
718 words, the key assumption that underlies the variational formulation on offer here is the
719 existence of an attracting set that underwrites non-equilibrium steady-state.

720 5.2 Extending Variational Principles to Open Systems

721 Because we have shown that the variational free energy minimization in active
722 inference is related to the variational principle of least action, it is worth pointing out
723 where these two approaches diverge. Due to the nature of the variational calculus and
724 least action principles, in which action is integrated over a time interval between fixed
725 time points, it is normally only applicable to closed systems – as opposed to biological
726 systems that operate far from thermodynamic equilibrium.

727 In order to measure action efficiency in complex open systems, the principle of least
728 action needs to be modified from the minimal action along a single, fixed trajectory, to
729 the minimum of the average action over an ensemble of trajectories within a certain
730 interval of time.

731 In open systems, there is a constant flow and change of the number of states and
732 constraints, as well as of the energy of the system itself. This will cause the system to
733 converge onto an attractor state, without ever truly reaching it, but instead to be in a
734 constant process of reorganization . [Georgiev, 2012].

735 The same is true for the simulations in this paper, where the system starts in a far
736 from equilibrium state, which necessitated the introduction of the time sensitivity τ .
737 Furthermore, while the variational free energy is minimized over time and the system
738 appears to approach an attractor state, partial information flow remains in the updating
739 of prior beliefs, largely due to the intrinsic random fluctuations ω of the external states.

740 5.3 Applicability of Bayesian Inference to Biological Systems

741 One central aspect of the modeling based on the Bayesian inference process
742 employed above is the updating of prior beliefs (that is the parameters of an agent's
743 internal model encoding its expectation of its environment) via evidence accumulation
744 through the Bayes theorem of (1), as dictated by ever changing active states which,
745 effectively, fulfil predictions. Because this process rest on the minimization of the
746 variational free energy and with it the divergence of prior belief and posterior density
747 introduced in (33), this necessarily implies an observable non-random exploratory
748 mechanism that can accumulate the evidence needed to update priors. For example, in
749 visual perception, saccadic eye movements have been identified and modeled as just
750 such an exploratory mechanism that accumulates model evidence efficiently [Friston
751 et al., 2012].

752 In this setting, actions are selected that minimize expected free energy, where
753 expected free energy features uncertainty reducing, information seeking aspects. In
754 non-neural biology, adaptation to environmental stresses have been shown to elicit an
755 exploratory response in gene expression, such as previously unexpressed exogenous
756 genes in rats following stress stimulation [Elgart et al., 2015]. Theoretical simulations
757 from the same group have shown that this compensation can – in theory – be explained
758 using random exploratory expression of genes until the correct gene is expressed [Soen
759 et al., 2015], [Schreier et al., 2017], but the question must be asked how efficient this
760 would be in the context of short term adaptation, and how negative effects resulting
761 from random expression of detrimental genes would be counterbalanced. Instead, we
762 hypothesize along the lines of Bayesian inference, that this gene expression is not
763 random, but follows distinct trajectories that are encoded by changes in active states of
764 the cell (e.g., protein translation, cytoskeletal rearrangement and membrane
765 permeability and receptor activity modifications).

766 In other words, we postulate that expression of exogenous or otherwise unexpected
767 genes is driven by a directed, explorative process where active states become expression
768 profiles that aim to minimize variational free energy through prior beliefs encoded by
769 the internal epigenetic states in the Bayesian sense as outlined above. If none of these

770 distinct trajectories are present, we would have to conclude that no Bayesian inference
771 process can take place on the level of gene expression in such an adaptation experiment
772 but would instead have to move towards an adaptation mechanism on a different
773 time-scale, such as its transient bioelectric states. As seen in the previous sections, the
774 same is true for prior beliefs (such as encoded by the epigenetic state of a cell), which
775 need to be able to be updated within a time window smaller than that of physiological
776 adaptation.

777 5.4 Predictive Capability of the Simulations

778 In our simulations, we were able to systematically perturb the overall morphology of
779 our model system without changing the internal, generative model of the constituent
780 cells; i.e., the gene regulatory networks that motivate the internal states. First, we
781 produced alterations of anterior-posterior polarity (i.e., two head or two tail regions),
782 which emulate phenotypes as inducible in planarian regeneration [Durant et al., 2017].
783 While the mechanism of the phenotype induced by transient bioelectric pattern
784 perturbations explored by Durant *et al.* was not explicitly used in this model, it is
785 worth pointing out that both leave the underlying, hardwired internal states – i.e., the
786 genetic level – unmodified, but instead work on the computational cellular processes
787 that encode map of the final target morphology [Levin, 2012b].

788 Second, we reproduced abnormal signaling and functional behavior of a single cell
789 within a cellular ensemble as a first step in cancer formation. We show that with simple
790 modifications of the inference process we can induce – and rescue – mispatterning of
791 these developmental and regenerative events – without changing the hard-wired
792 generative model of the cell as determined by its DNA. We conclude that macro- onto
793 micro-scale feedback during development and regeneration – especially considering the
794 capability of developing tissue to dynamically adapt to changes in its environment –
795 implies the need for active inference on a cellular level, and that the variational
796 formalism explored in this work provides us with the means to predict and control its
797 outcomes.

798 5.5 Concluding Remarks

799 A major challenge in current attempts to control the morphogenetic outcomes in
800 developmental or regenerative biological systems is the quantitative modeling of how the
801 signaling and sensing activities of individual cells are coordinated and regulated to
802 result in large-scale anatomical patterns that enable robust structure and
803 function [Levin, 2012b], [Gilbert and Sarkar, 2000].

804 An important gap in the field is that the complexity and non-equilibrium nature of
805 the biological systems investigated have made the computation of the flow of states over
806 time – and thereby the control of that flow to a different stable attractor state
807 corresponding to a desired morphogenetic outcome – near impossible.

808 Here, we show how a variational free energy formulation – which casts morphogenesis
809 as a (Bayesian) inference process – allows us to control specific morphogenesis outcomes
810 through manipulations to the external biophysics; by providing the fundamental insight
811 and modeling capability of how these biophysical, morphogenetic fields [Levin,
812 2012b], [Goodwin, 2000] are interpreted by individual cells and used to coordinate on a
813 macroscopic level. Notably, this capability is achieved without changing the implicit
814 generative model of a cell as specified, for example, by its DNA. Therefore, this
815 formalism offers a new road map for understanding developmental change in evolution
816 and for designing new interventions in regenerative medicine settings, where
817 system-level results of interventions on the genomic level hard to predict.

818 Equipped with these proof-of-principle results, we can now explore a larger
819 repertoire of manipulations that speak to key empirical phenomena in developmental
820 and regenerative biology. Crucially, the challenge will be to write – and test at the
821 bench – a generative model for a real developmental, regenerative, or aberrant biological
822 system, where realistic biophysical parameters can be fed into an experimentally
823 tractable *in vivo* model for unprecedented rational control of growth and form [Pezzulo
824 and Levin, 2015], [Pezzulo and Levin, 2016].

825 References

- 827 Adams et al., 2013. Adams, R. A., Shipp, S., and Friston, K. J. (2013). Predictions
828 not commands: active inference in the motor system. *Brain Structure and Function*,
829 218(3):611–643.
- 830 Arfken and Weber, 1995. Arfken, G. and Weber, H. (1995). Mathematical methods
831 for physicists. *Academic Press*, page 612.
- 832 Arnold, 1995. Arnold, L. (1995). *Random dynamical systems*, pages 1–43. Springer
833 Berlin Heidelberg, Berlin, Heidelberg.
- 834 Baluška and Levin, 2016. Baluška, F. and Levin, M. (2016). On having no head:
835 cognition throughout biological systems. *Frontiers in psychology*, 7:902.
- 836 Banerjee, 2014. Banerjee, N. (2014). Neurotransmitters in alcoholism: A review of
837 neurobiological and genetic studies. *Indian journal of human genetics*, 20(1):20.
- 838 Barrett and Simmons, 2015. Barrett, L. F. and Simmons, W. K. (2015).
839 Interoceptive predictions in the brain. *Nature Reviews Neuroscience*, 16:419.
- 840 Boltzmann, 2009. Boltzmann, L. (2009). *Vorlesungen uber Gastheorie*. BiblioBazaar,
841 LLC.
- 842 Buckley et al., 2017. Buckley, C. L., Kim, C. S., McGregor, S., and Seth, A. K.
843 (2017). The free energy principle for action and perception: A mathematical review.
844 *Journal of Mathematical Psychology*, 81:55–79.
- 845 Bugaj et al., 2017. Bugaj, L. J., O’Donoghue, G. P., and Lim, W. A. (2017).
846 Interrogating cellular perception and decision making with optogenetic tools. *J Cell*
847 *Biol*, 216(1):25–28.
- 848 Chambon, 1996. Chambon, P. (1996). A decade of molecular biology of retinoic acid
849 receptors. *The FASEB Journal*, 10(9):940–954.
- 850 Clark, 2017. Clark, A. (2017). How to knit your own Markov blanket.
- 851 Corbetta and Shulman, 2002. Corbetta, M. and Shulman, G. L. (2002). Control of
852 goal-directed and stimulus-driven attention in the brain. *Nature Reviews*
853 *Neuroscience*, 3:201.
- 854 Crauel and Flandoli, 1994. Crauel, H. and Flandoli, F. (1994). Attractors for
855 random dynamical systems. *Probability Theory and Related Fields*, 100(3):365–393.
- 856 Desimone and Duncan, 1995. Desimone, R. and Duncan, J. (1995). Neural
857 mechanisms of selective visual attention. *Annual Review of Neuroscience*,
858 18(1):193–222.

859 Dinner et al., 2000. Dinner, A. R., Šali, A., Smith, L. J., Dobson, C. M., and
860 Karplus, M. (2000). Understanding protein folding via free-energy surfaces from
861 theory and experiment. *Trends in biochemical sciences*, 25(7):331–339.

862 Durant et al., 2016. Durant, F., Lobo, D., Hammelman, J., and Levin, M. (2016).
863 Physiological controls of large-scale patterning in planarian regeneration: a
864 molecular and computational perspective on growth and form. *Regeneration*,
865 3(2):78–102.

866 Durant et al., 2017. Durant, F., Morokuma, J., Fields, C., Williams, K., Adams,
867 D. S., and Levin, M. (2017). Long-term, stochastic editing of regenerative anatomy
868 via targeting endogenous bioelectric gradients. *Biophys J*, 112(10):2231–2243.

869 El Kaabouchi and Wang, 2015. El Kaabouchi, A. and Wang, Q. A. (2015). Least
870 action principle and stochastic motion: a generic derivation of path probability. In
871 *Journal of Physics: Conference Series*, volume 604, page 012011. IOP Publishing.

872 Elgart et al., 2015. Elgart, M., Snir, O., and Soen, Y. (2015). Stress-mediated tuning
873 of developmental robustness and plasticity in flies. *Biochimica et Biophysica Acta*
874 *(BBA)-Gene Regulatory Mechanisms*, 1849(4):462–466.

875 England, 2015. England, J. L. (2015). Dissipative adaptation in driven self-assembly.
876 *Nature nanotechnology*, 10(11):919.

877 Evans and Searles, 2002. Evans, D. J. and Searles, D. J. (2002). The fluctuation
878 theorem. *Advances in Physics*, 51(7):1529–1585.

879 Friston, 2013. Friston, K. (2013). Life as we know it. *Journal of the Royal Society*,
880 *Interface / the Royal Society*, 10(86):20130475.

881 Friston et al., 2012. Friston, K., Adams, R. A., Perrinet, L., and Breakspear, M.
882 (2012). Perceptions as hypotheses: saccades as experiments. *Front Psychol*, 3:151.

883 Friston et al., 2017. Friston, K., FitzGerald, T., Rigoli, F., Schwartenbeck, P., and
884 Pezzulo, G. (2017). Active inference: A process theory. *Neural Comput*, 29(1):1–49.

885 Friston and Kiebel, 2009. Friston, K. and Kiebel, S. (2009). Predictive coding under
886 the free-energy principle. *Philosophical Transactions of the Royal Society B:*
887 *Biological Sciences*, 364(1521):1211–1221.

888 Friston et al., 2015. Friston, K., Levin, M., Sengupta, B., and Pezzulo, G. (2015).
889 Knowing one ’ s place : a free-energy approach to pattern regulation. 3.

890 Friston et al., 2007. Friston, K., Mattout, J., Trujillo-Barreto, N., Ashburner, J., and
891 Penny, W. (2007). Variational free energy and the laplace approximation.
892 *Neuroimage*, 34(1):220–234.

893 Friston et al., 2010. Friston, K., Stephan, K., Li, B., and Daunizeau, J. (2010).
894 Generalised Filtering. *Mathematical Problems in Engineering*, 2010:1–34.

895 Friston, 2008. Friston, K. J. (2008). Variational filtering. *Neuroimage*, 41(3):747–766.

896 Friston et al., 2008. Friston, K. J., Trujillo-Barreto, N., and Daunizeau, J. (2008).
897 DEM: a variational treatment of dynamic systems. *Neuroimage*, 41(3):849–885.

898 Georgiev and Georgiev, 2002. Georgiev, G. and Georgiev, I. (2002). The least action
899 and the metric of an organized system. *Open systems & information dynamics*,
900 9(4):371.

-
- 901 Georgiev, 2012. Georgiev, G. Y. (2012). A quantitative measure, mechanism and
902 attractor for self-organization in networked complex systems. In *International*
903 *Workshop on Self-Organizing Systems*, pages 90–95. Springer.
- 904 Georgiev and Chatterjee, 2016. Georgiev, G. Y. and Chatterjee, A. (2016). The road
905 to a measurable quantitative understanding of self-organization and evolution. In
906 *Evolution and Transitions in Complexity*, pages 223–230. Springer.
- 907 Georgiev et al., 2017. Georgiev, G. Y., Chatterjee, A., and Iannacchione, G. (2017).
908 Exponential self-organization and moore's law: Measures and mechanisms.
909 *Complexity*, 2017.
- 910 Georgiev et al., 2015. Georgiev, G. Y., Henry, K., Bates, T., Gombos, E., Casey, A.,
911 Daly, M., Vinod, A., and Lee, H. (2015). Mechanism of organization increase in
912 complex systems. *Complexity*, 21(2):18–28.
- 913 Gilbert and Sarkar, 2000. Gilbert, S. F. and Sarkar, S. (2000). Embracing
914 complexity: organicism for the 21st century. *Developmental dynamics: an official*
915 *publication of the American Association of Anatomists*, 219(1):1–9.
- 916 Gilman, 1987. Gilman, A. G. (1987). G proteins: transducers of receptor-generated
917 signals. *Annual review of biochemistry*, 56(1):615–649.
- 918 Goodwin, 2000. Goodwin, B. C. (2000). The life of form. emergent patterns of
919 morphological transformation. *Comptes Rendus de l'Académie des Sciences-Series*
920 *III-Sciences de la Vie*, 323(1):15–21.
- 921 Hohwy, 2016. Hohwy, J. (2016). The self-evidencing brain. *Noûs*, 50(2):259–285.
- 922 Imoto et al., 2001. Imoto, S., Goto, T., and Miyano, S. (2001). Estimation of genetic
923 networks and functional structures between genes by using bayesian networks and
924 nonparametric regression. In *Biocomputing 2002*, pages 175–186. World Scientific.
- 925 Lammert et al., 2012. Lammert, H., Noel, J. K., and Onuchic, J. N. (2012). The
926 dominant folding route minimizes backbone distortion in sh3. *PLoS computational*
927 *biology*, 8(11):e1002776.
- 928 Levin, 2012a. Levin, M. (2012a). Molecular bioelectricity in developmental biology:
929 new tools and recent discoveries: control of cell behavior and pattern formation by
930 transmembrane potential gradients. *Bioessays*, 34(3):205–217.
- 931 Levin, 2012b. Levin, M. (2012b). Morphogenetic fields in embryogenesis,
932 regeneration, and cancer: non-local control of complex patterning. *Biosystems*,
933 109(3):243–261.
- 934 Levin et al., 2019. Levin, M., Pietak, A. M., and Bischof, J. (2019). Planarian
935 regeneration as a model of anatomical homeostasis: recent progress in biophysical
936 and computational approaches. In *Seminars in cell & developmental biology*,
937 volume 87, pages 125–144. Elsevier.
- 938 Lijun et al., 2008. Lijun, Q., Haixin, W., and Dougherty, E. R. (2008). Inference of
939 noisy nonlinear differential equation models for gene regulatory networks using
940 genetic programming and kalman filtering. *IEEE Transactions on Signal Processing*,
941 56(7):3327–3339.
- 942 Longo and Montévil, 2013. Longo, G. and Montévil, M. (2013). Extended criticality,
943 phase spaces and enablement in biology. *Chaos Solitons and Fractals*, 55:64–79.

944 Lyapunov, 1992. Lyapunov, A. M. (1992). The general problem of the stability of
945 motion. *International journal of control*, 55(3):531–534.

946 Mahas et al., 2018. Mahas, A., Neal Stewart, C., and Mahfouz, M. M. (2018).
947 Harnessing CRISPR/Cas systems for programmable transcriptional and
948 post-transcriptional regulation. *Biotechnology Advances*, 36(1):295–310.

949 Marreiros et al., 2009. Marreiros, A. C., Kiebel, S. J., Daunizeau, J., Harrison, L. M.,
950 and Friston, K. J. (2009). Population dynamics under the laplace assumption.
951 *Neuroimage*, 44(3):701–714.

952 Mawhin, 2015. Mawhin, J. (2015). Alexandr Mikhailovich Liapunov, The general
953 problem of the stability of motion (1892). *ResearchGate*.

954 Moore et al., 2017. Moore, D., Walker, S. I., and Levin, M. (2017). Cancer as a
955 disorder of patterning information: computational and biophysical perspectives on
956 the cancer problem. *Convergent Science Physical Oncology*, 3(4):043001.

957 Moutoussis et al., 2014. Moutoussis, M., Fearon, P., El-Deredy, W., Dolan, R. J.,
958 and Friston, K. J. (2014). Bayesian inferences about the self (and others): A review.
959 *Consciousness and cognition*, 25:67–76.

960 Mutoh et al., 2012. Mutoh, H., Akemann, W., and Knöpfel, T. (2012). Genetically
961 engineered fluorescent voltage reporters. *ACS Chemical Neuroscience*, 3(8):585–592.

962 Noor et al., 2012. Noor, A., Serpedin, E., Nounou, M., and Nounou, H. N. (2012).
963 Inferring gene regulatory networks via nonlinear state-space models and exploiting
964 sparsity. *IEEE/ACM Trans Comput Biol Bioinform*, 9(4):1203–1211.

965 Pezzulo and Levin, 2015. Pezzulo, G. and Levin, M. (2015). Re-membering the body:
966 applications of computational neuroscience to the top-down control of regeneration
967 of limbs and other complex organs. *Integrative Biology*, 7(12):1487–1517.

968 Pezzulo and Levin, 2016. Pezzulo, G. and Levin, M. (2016). Top-down models in
969 biology: explanation and control of complex living systems above the molecular
970 level. *Journal of the Royal Society Interface*, 13(124):20160555.

971 Prigogine, 1978. Prigogine, I. (1978). Time, structure, and fluctuations. *Science*,
972 201(4358):777–785.

973 Rosen, 2012. Rosen, R. (2012). Anticipatory systems. In *Anticipatory systems*, pages
974 313–370. Springer.

975 Schreier et al., 2017. Schreier, H. I., Soen, Y., and Brenner, N. (2017). Exploratory
976 adaptation in large random networks. *Nature communications*, 8:14826.

977 Seifert, 2012. Seifert, U. (2012). Stochastic thermodynamics, fluctuation theorems
978 and molecular machines. *Reports on Progress in Physics*, 75(12):126001.

979 Soen et al., 2015. Soen, Y., Knafo, M., and Elgart, M. (2015). A principle of
980 organization which facilitates broad lamarckian-like adaptations by improvisation.
981 *Biology direct*, 10(1):68.

982 Ungerleider and Leslie, 2000. Ungerleider, S. K. and Leslie, G. (2000). Mechanisms
983 of visual attention in the human cortex. *Annual Review of Neuroscience*,
984 23(1):315–341.

-
- 985 V. Sekar et al., 2011. V. Sekar, T., Dhanabalan, A., and Paulmurugan, R. (2011).
986 Imaging cellular receptors in breast cancers: An overview. *Current Pharmaceutical*
987 *Biotechnology*, 12(4):508–527.
- 988 Yuan et al., 2014. Yuan, R.-S., Ma, Y.-A., Yuan, B., and Ao, P. (2014). Lyapunov
989 function as potential function: A dynamical equivalence. *Chinese Physics B*, 23(1).